34th Annual International Conference of the IEEE EMBS
San Diego, California USA, 28 August - 1 September, 2012

Evaluations of Sparse Source Imaging and Minimum Norm Estimate Methods in both Simulation and Clinical MEG Data*

Min Zhu, *Student Member, IEEE*, Wenbo Zhang, Deanna Dickens and Lei Ding, *Member, IEEE*

***Abstract*—The aim of the present study is to evaluate the capability of a recently proposed l^1-norm based regularization method, named as variation-based sparse cortical current density (VB-SCCD) algorithm, in estimating location and spatial coverage of extensive brain sources. Its performance was compared to the conventional minimum norm estimate (MNE) using both simulations and clinical interictal spike MEG data from epilepsy patients. Four metrics were adopted to evaluate two regularization methods for EEG/MEG inverse problems from different aspects in simulation study. Both methods were further compared in reconstructing epileptic sources and validated using results from clinical diagnosis. Both simulation and experimental results suggest VB-SCCD has better performance in localization and estimation of source extents, as well as less spurious sources than MNE, which makes it a promising noninvasive tool to assist presurgical evaluation for surgical treatment in epilepsy patients.**

I. Introduction

Interictal spikes recorded in electroencephalography (EEG) and/or magnetoencephalography (MEG) play an important role in localizing epileptiform foci in pre-surgical evaluation for medically refractory partial epilepsy patients. It has been suggested by intracranial recording that extensive synchronous cortical activations (>6 cm^2) are required for scalp detectable spikes [1]. Cortical current density (CCD) models have been widely used for modeling extensive brain activities with dipolar elements distributed on a two-dimensional cortical mesh representing the gray/white matter interface [2]. Whereas, the large number of parameters (~10,000) to be estimated in CCD models aggravates the ill-poseness in solving EEG/MEG inverse problems from limited number of measurements (~100).

Regularization schemes are usually adopted to obtain a unique solution by placing proper priors [3]. Some commonly used priors can be classified into two types: (1) anatomical (or spatial) priors, such as constraining dipole locations and orientations with cortical spatial structure [4,5]; (2) functional priors, which can be data driven using Bayesian theory [6] or most commonly based on some neurophysiological assumptions, such as minimal overall energy of sources (l^2-norm) [3,7], maximal sparseness of sources (l^1-norm) [8], or smoothness in temporal transactions [5]. Anatomical and functional priors can be utilized separately [7-8] or combined together [4,5,6,9].

Recently, we proposed a novel regularization scheme, i.e. variation-based sparse cortical current density (VB-SCCD) method [10], to combine anatomical prior as local spatial homogeneousness and functional prior as sparseness. The local spatial homogeneous was achieved by minimizing variations between neighboring elements in CCD models. Attaining sparseness of variations using l^1-norm is to ensure a small amount of variations happened on boundaries of active and non-active areas. To evaluate the performance of this novel regularization method, previously simulation study [10] conducted a comparison between VB-SCCD and variants of l^2-norm minimum norm estimate (MNE) [7], such as one implemented with source depth weights, i.e., weighted MNE (wMNE) [3], and others with the use of local smoothness, e.g., cortical low resolution electromagnetic tomography (cLORETA) [3]. The results showed an enhanced ability of VB-SCCD in estimating extensive sources than other two methods. Although introduced weights in wMNE and cLORETA might compensate bias due to the source depth, they are highly dependent on quality of head volume models, which may result in reduced performance when segmentations of head volume conductors from anatomical magnetic resonance imaging (MRI) data are not perfect [11]. Moreover, the evaluation metric adopted in the above simulation study, i.e., area under receiver operating characteristic curve (AUC) [12], only assessed accuracy of spatial source coverage, but neglected evaluations of global energy, locations of maxima, and spatial blurredness of estimated sources, which have been suggested of importance in evaluating performance of inverse methods [12-14].

In the present study, we further investigated the performance of this l^1-norm based regularization method (i.e., VB-SCCD) with comparison to conventional l^2-norm MNE using multiple metrics. We further extended comparison studies from simulated data to empirical data of interictal MEG recordings from partial epilepsy patients. In addition to the previously used assessment criteria (i.e., AUC), other three metrics were introduced. Validations and comparisons of both methods in clinical data were performed in reference to outcomes from clinic diagnosis.

II. Method

A. Forward model

According to Maxwell's equations, magnetic fields φ measured at M sensors are linear functions of N dipole

* The work was supported in part by OCAST HR09-125S, NSF CAREER ECCS-0955260, and DOT-FAA10-G-008.

M. Zhu is with the School of Electrical and Computer Engineering, University of Oklahoma, Norman, OK 73019 (phone: 4053253774; fax: 4053257066; e-mail: Min.Zhu-1@ou.edu).

W. Zhang (email: wzhang@mnepilepsy.net) and D. Dickens (email: ddickens@mnepilepsy.net) are with the Minnesota Epilepsy Group, St. Paul, MN 55102.

L. Ding is with the School of Electrical and Computer Engineering and Center for Biomedical Engineering, University of Oklahoma, Norman, OK 73019 (e-mail: leiding@ou.edu).

amplitudes s on the cortex [15]:

$$\varphi = \mathbf{L}s + n \,. \tag{1}$$

where $\mathbf{L}$ is the lead field and n is addictive noise. The number of dipoles N is usually much larger than the number of measurements M, which makes the problem highly underdetermined. Regularization schemes are thus introduced to search for a unique solution under proper priors.

B. Inverse model

Classic MNE [7] is the most commonly used l^2-norm regularization scheme to search for a solution with minimum energy:

$$\min \|s\|_2 \quad \text{subject to} \quad \|\varphi - \mathbf{L}s\|_2 \le \varepsilon \,. \tag{2}$$

where ε is the regularization parameter to control noise.

In VB-SCCD [10], it proposes an l^1-norm regularization scheme to search for a current distribution with minimum variations:

$$\min \|\mathbf{V}s\|_1 \quad \text{subject to} \quad \|\varphi - \mathbf{L}s\|_2 \le \varepsilon \,. \tag{3}$$

The operator $\mathbf{V}$ is designed to calculate the variations between two neighboring elements:

$$\mathbf{V} = \begin{bmatrix} v_{11} & v_{12} & \cdots & v_{1N} \\ v_{21} & v_{22} & \cdots & v_{2N} \\ \vdots & \vdots & \ddots & \vdots \\ v_{P1} & v_{P2} & \cdots & v_{PN} \end{bmatrix}$$

$$\begin{cases} v_{ij} = 1; v_{ik} = -1; & \text{if triangles } j,k \text{ share the same edge } i \\ v_{ij} = 0; & \text{otherwise} \end{cases}$$

where P is the total number of triangle edges.

The constrained optimization problems in both (2) and (3) can be solved by second order cone programming (SOCP) [16], which has been integrated in a Matlab package called Self-Dual-Minimization (SeDuMi).

C. Simulation protocol

Anatomical MRI data of an average subject were from FreeSurfer's example sets (http://surfer.nmr.mgh.harvard.edu) were used in simulations. Boundary element (BE) head model was segmented from the scalp, skull and brain surfaces and tessellated into triangular meshes with in total 6144 triangles using FreeSurfer software [17]. Conductivities for the scalp, skull and brain were assigned to be 0.33/Ω.m, 0.0165/Ω.m, and 0.33/Ω.m respectively [18]. Cortical surface was numerically tessellated from the interface between gray matter and white matter as a high-resolution triangular mesh (40960 triangles) segmented using the same software to form the CCD model, and the source space was modeled as current dipoles located at center of each triangle in CCD model and aligned to local norms. To simulate extensive cortical sources, cortical patches were generated by randomly picking up a seed triangle and iteratively adding neighboring triangles. Dipole amplitudes inside cortical patches were simulated as the product of triangular areas and dipole moment density (i.e.100 pAm/mm^2). To test the robustness of inverse methods in recovering simultaneously activated sources, simulations were repeated 200 times with two sources of around 7 cm^2 from randomly selected locations. Measurements were simulated based on a 148-channel MEG system and contaminated with Gaussian white noise of signal to noise ratio (SNR) equal 20 dB.

Multiple metrics were used to evaluate the performance of MNE and VB-SCCD. The AUC metric, derived from receiver operating characteristic (ROC) curves, is to assess the detection accuracy of spatial source coverage [10]. In the present study, a "hard" AUC was adopted rather than the "soft" AUC in [12] to obtain less biased false positive rate in ROC analysis. The spatial dispersion (SD) was originally related to width of point spread function (PSF) in resolution matrix derived from linear (i.e., l^2-norm) estimators [13], and further extended to nonlinear (i.e., l^1-norm) estimators by measuring blurredness between true sources to estimated sources [14]. The distance of localization error (DLE) was defined as averaged distance from true sources to maximal source estimate [14]. Both SD and DLE measured concentricity of estimated sources referring to true sources. While DLE only assesses the displacement of maxima, SD can reflect both displacement and spatial blurring. To avoid bias in estimating SD in situations that small background fluctuations in estimates far from true source locations led to overwhelming SD values, 10% of global maximum was applied to threshold small estimates. The mean square error (MSE) [12] was also used to evaluate recovery of global energy.

D. Experiment protocol

To further evaluate both methods, MEG interictal spikes (IISs) were collected from three patients with medically refractory partial epilepsy. Individual BE head models and cortex models were obtained by segmenting T1-weighted structural MRI data for each patient using BrainSuite software [19]. Spontaneous MEG was recorded using 148-channel Magnes WH2500 neuromagnetometer array (4-D Neuroimaging, San Diego, CA, USA). Reconstructed epileptic foci were then compared with clinic diagnosis, MRI lesions, as well as surgical resections and post-surgery outcomes when possible.

III. Results

A. Simulation results

In Fig. 1(a), both MNE and VB-SCCD indicates high detection accuracies by AUC median values exceeding 0.8. However, VB-SCCD shows a slightly higher AUC than MNE (while not of statistical significance). Both SD and DLE of VB-SCCD are significantly lower than those of MNE ($p<10^{-11}$), indicating that VB-SCCD has less blurredness and displacement in reconstructing extensive cortical sources. VB-SCCD also shows a better ability in recovering global energy, indicated by a significant lower MSE value ($p<0.0275$). It is observed that MNE highly underestimates dipole amplitudes, leading MSE value close to 1. To better

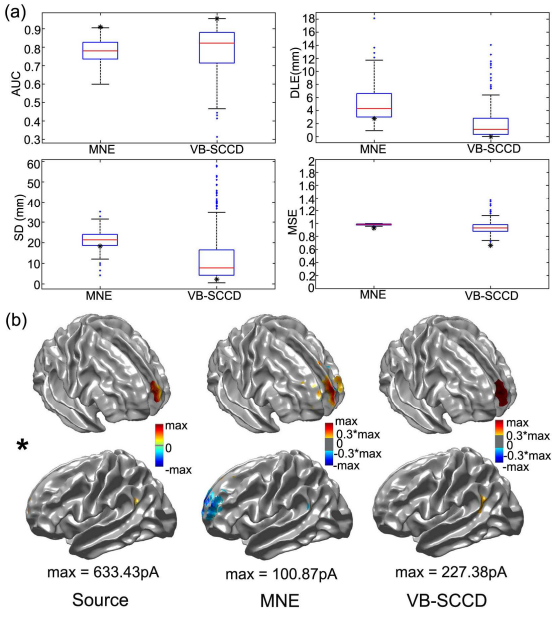

Figure 1. (a). Whisker plots of AUC, DLE, SD, and RE from MNE and VB-SCCD. "*" indicates metric values for the given example in (b). (b) One example of simulated sources and estimated sources by MNE and VB-SCCD.

visualize the difference between reconstructions from both MNE and VB-SCCD, one example was provided in Fig. 1(b) with simulated mesial frontal and posterior temporal sources. Although both two methods have high AUC values (>0.9), sources in the mesial frontal cortex were estimated by MNE with spurious source distributed on pre-frontal areas, while source estimated by VB-SCCD was continuously distributed within mesial frontal region with extensive spatial coverage much more similar to simulated one. This observation was collaborated by higher values in SD and DLE for MNE, but not in AUC. It is also observed that positive source within sulcus was mostly often reconstructed by MNE with positive currents on one side wall of sulcus and negative currents on the other side, while VB-SCCD did not show such spurious reconstructions. Dipole amplitudes were underestimated greatly by both methods (simulated: 633.43pA, MNE: 100.87pA, and VB-SCCD: 227.38pA), while it was more significant in MNE than VB-SCCD.

B. Experiment results

Fig. 2 shows one example of IISs from Patient 1. The spatial distributions of magnetic fields in the sensor space indicate possible source origins from the right temporal lobe. Moving from the sensor space to the source space, the sources estimated by MNE mainly disperse on the right temporal areas with a spatially extensive coverage of middle and inferior temporal cortices, and extra-temporal sources are also observed across medial frontal and parietal cortices. The sources estimated from VB-SCCD indicate confined activations located on the right superior temporal cortex extending into the lateral sulcus. Moreover, the strength of cortical activations increases before reaching the IIS peak and then decreases. The pre-surgical diagnosis for this patient suggested extensive MRI lesions located within the right lateral fissure. Source estimates from VB-SCCD are more consistent with clinical diagnosis than MNE in terms of both

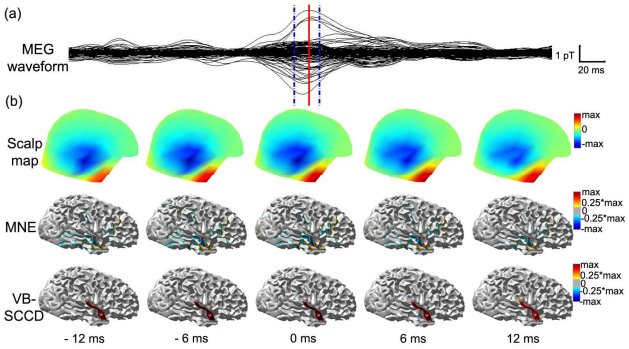

Figure 2. Patient 1. (a) MEG sensor waveforms of an IIS. The red solid line indicates IIS peak and two blue dashed line indicates 12 ms before and 12 ms after the peak. (b) MEG scalp maps and estimated cortical sources of the IIS by MNE and VB-SCCD.

location and spatial coverage.

One example of IISs from Patient 2 is shown in Fig. 3. It is observed that magnetic scalp maps indicated a focus on the right frontal region. The sources estimated from MNE mainly disperse on the right medial frontal cortex with inflow currents indicated by negative values in Fig. 3(b), while the sources estimated by VB-SCCD locate on the right pre-frontal lobe covering part of orbital frontal cortices with outflow currents, as well as on the middle frontal and inferior parietal cortices with inflow currents. Moreover, the sequence of source estimates from VB-SCCD reveals a dynamic increase of activation strength before the IIS peak and a fast decrease after the IIS peak in milliseconds. This patient had multiple MRI lesions located on the anterior and medial sections of right frontal regions, which were consistent with VB-SCCD estimates. However, the anterior frontal origin is missed in MNE estimates.

Fig. 4 shows one example IIS from Patient 3. The magnetic scalp maps indicate a left focus on temporal areas. The sources estimated by MNE mainly disperse on the left superior temporal and medial frontal cortices. The sources reconstructed by VB-SCCD reveal a dynamic propagation pattern from the posterior portion of left lateral fissure (related to auditory process) to the inferior frontal cortex (related to language process). This patient, who was diagnosed as Landau-Kleffner syndrome (LKS) [20], didn't have any visible MRI lesions. However, the coverage of auditory and language cortices in VB-SCCD source estimates

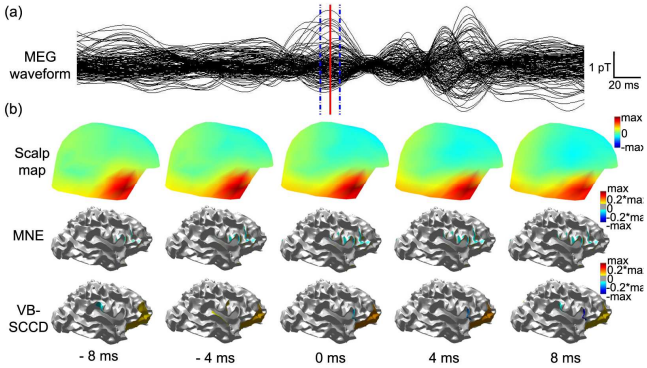

Figure 3. Patient 2. (a) MEG sensor waveforms of an IIS. (b) MEG scalp maps and reconstructed cortical sources of the IIS by MNE and VB-SCCD.

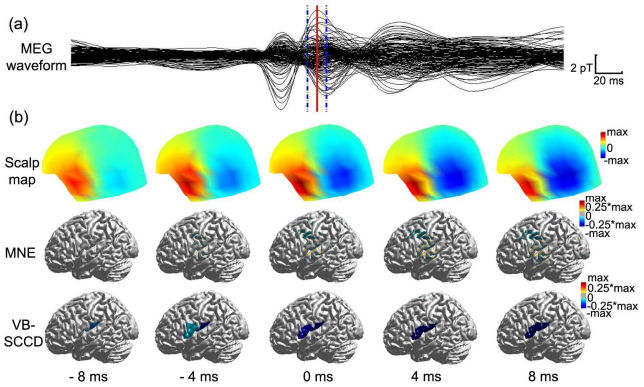

Figure 4. Patient 3. (a) MEG sensor waveforms of an IIS. (b) MEG scalp maps and reconstructed cortical sources of the IIS by MNE and VB-SCCD.

are consistent with the loss of ability of LKS patients in understanding and expressing language.

IV. Discussion

In the present study, multiple assessment metrics (i.e., AUC, DLE, SD and MSE) were used to evaluate the performance of regularization methods (i.e., MNE and VB-SCCD) in simulations. All those four metrics suggested the better performance of VB-SCCD than MNE in reconstructing extensive cortical sources. Meanwhile, the difference between MNE and VB-SCCD in AUC metric is not as significant as in DLE, SD and MSE. These data indicate that source localization and estimation accuracies should be assessed in multiple aspects and single evaluation metric might not be able to perform complete assessments. Furthermore, direct visualizations of estimated sources also provide a useful mean to assess inverse estimation results. One simulation example provided in Fig. 2 further indicates the better performance of VB-SCCD in reconstructing extensive cortical sources than MNE, while such difference is not well captured in the metric of AUC.

VB-SCCD reveals the better ability in recovering extensive cortical sources without spurious sources, while MNE often generates such spurious sources in surrounding cortical areas. The same phenomenon is also observed in estimating IIS sources in epilepsy patients (such as in Fig. 2). Spurious sources in surrounding areas by l^2-norm based estimators have been previously reported in [12]. The ability of VB-SCCD in suppressing spurious sources might attribute to seeking sparseness using l^1-norm.

In the analysis of clinical data, VB-SCCD also indicates more consistent sources than MNE as compared to results from clinical diagnosis in terms of locations, spatial coverage, and temporal dynamics. These facts suggested that the novel regularization approach for EEG/MEG inverse problems is promising to non-invasively identify epileptic origins in pre-surgical evaluation for epilepsy patients. Stable source dynamics suggested by VB-SCCD further provide a useful window on inspecting time courses of epileptic sources. Such information can provide millisecond level of resolutions to understand the formation and propagation of epileptic activities, which is extremely valuable in unveiling underlying mechanisms of epilepsy.

Acknowledgment

We thank Mr. Joel Landsteiner from Minnesota Epilepsy Group for his technical assistance.

References

[1] R. Cooper, A. L. Winter, H. J. Crow and W. G. Walter, "Comparison of subcortical, cortical and scalp activity using chronically indwelling electrodes in man," *Electroencephalogr and Clin Neurophysiol,* vol. 18, pp. 217-228, 1965.

[2] A. M. Dale and M. I. Sereno, "Improved localization of cortical activity by combining EEG and MEG with MRI cortical surface reconstruction," *J Cogn Neurosci* vol. 5, pp. 162-176, 1993.

[3] R. Grech, T. Cassar, J. Muscat, K. P. Camilleri, S. G. Fabri, M. Zervakis, P. Xanthopoulos, V. Sakkalis and B. Vanrumste, "Review on solving the inverse problem in EEG source analysis," *J Neuroeng Rehabil*, vol. 5, pp. 5-25, Nov. 2008.

[4] C. Phillips, M. D. Rugg and K. J. Friston, "Anatomically Informed Basis Functions for EEG Source Localization: Combining Functional and Anatomical Constraints," *NeuroImage,* vol. 16, pp. 678-695, 2002.

[5] S. Baillet and L. Garnero, "A Bayesian Approach to Introducing Anatomo-Functional Priors in the EEG/MEG Inverse Problem," *IEEE Trans. Biomed Eng,* vol. 44, pp. 374-385, 1997.

[6] N. J. Trujillo-Barreto, E. Aubert-Vázquez, and W. D. Penny, "Bayesian M/EEG source reconstruction with spatio-temporal priors," *NeuroImage,* vol. 39, pp. 318-335, 2008.

[7] M. S. Hämäläinen and R. J. Ilmoniemi, "Interpreting measured magnetic fields of the brain: minimum norm estimates," *Med Biol Eng Comput,* vol. 32, pp. 35-42, 1994.

[8] K. Uutela, M. S. Hämäläinen, E. Somersalo, "Visualization of magnetoencephalographic data using minimum current estimates," *NeuroImage,* vol. 3S, p. 168, 1999.

[9] K. J. Friston, L. M. Harrison, J. Daunizeau, *et al.*, "Multiple sparse priors for the M/EEG inverse problem," *NeuroImage,* vol. 39, pp. 1104-1120, 2008.

[10] L. Ding, "Reconstructing cortical current density by exploring sparseness in the transform domain," *Phys Med Biol*, vol. 54, pp. 2683-2697, 2009.

[11] J. C. Mosher, R. M. Leahy, and P. S. Lewis, "EEG and MEG: forward solutions for inverse methods," *IEEE Trans. Biomed Eng,* vol. 46, pp. 245-259, 1999.

[12] C. Grova, J. Daunizeau, J. M. Lina, C. G. Bénar, H. Benali, and J. Gotman, "Evaluation of EEG localization methods using realistic simulations of interictal spikes," *NeuroImage,* vol. 29, pp. 734-753, 2006.

[13] A. Molins, S. M. Stufflebeam, E. N. Brown and M. S. Hämäläinen, "Quantification of the benefit from integrating MEG and EEG data in minimum ℓ2-norm estimation," *NeuroImage*, vol. 42, pp. 1069-1077, Sep. 2008.

[14] W.-T. Chang, A. Nummenmaa, J.-C. Hsieh, and F.-H. Lin, "Spatially sparse source cluster modeling by compressive neuromagnetic tomography," *NeuroImage,* vol. 53, pp. 146-160, 2010.

[15] P. L. Nunez, *Electric field of the brain*. London, Oxford University Press, 1981.

[16] S. Boyd and L. Vandenberghe, *Convex Optimization*. United Kingdom: Cambridge University Press, 2004.

[17] A. M. Dale, B. Fischl, and M. I. Sereno, "Cortical surface-based analysis," *NeuroImage,* vol. 9, pp. 179-194, 1999.

[18] Y. Lai, W. van Drongelen, L. Ding, K. E. Hecox, V. L. Towle, D. M. Frim and B. He, "Estimation of in vivo human brain-to-skull conductivity ratio from simultaneous extra- and intra-cranial electrical potential recordings," *Clin Neurophysiol*, vol. 116, pp. 456-465, Feb. 2005.

[19] D. W. Shattuck and R. M. Leahy, "Brainsuite: an automated cortical surface identification tool," *Med Image Anal*, vol. 8, pp. 129-142, Jun. 2002.

[20] W. M. Landau and F. R. Kleffner, "Syndrome of aquired aphasia with convulsive disorder in children," *Neurology,* vol. 7, pp. 520-530, 1957.